Liquid Crystals
Publication details, including instructions for authors and subscription information:
http://www.informaworld.com/smpp/title~content=t713926090

Optimisation of electrode structure to improve the electro-optic characteristics of liquid crystal display based on the Kerr effect

Sukin Yoon[a]; Miyoung Kim[a]; Min Su Kim[a]; Byeong Gyun Kang[a]; Mi-Kyung Kim[a]; Anoop Kumar Srivastava[a]; Seung Hee Lee[a]; Zhibing Ge[b]; Linghui Rao[b]; Sebastian Gauza[b]; Shin-Tson Wu[b]
[a] Polymer BIN Fusion Research Center, Department of Polymer Nano Science Engineering, Chonbuk National University, Chonju, Chonbuk, Korea [b] College of Optics and Photonics, University of Central Florida, Orlando, FL, USA

Online publication date: 11 February 2010

To cite this Article Yoon, Sukin , Kim, Miyoung , Su Kim, Min , Gyun Kang, Byeong , Kim, Mi-Kyung , Kumar Srivastava, Anoop , Hee Lee, Seung , Ge, Zhibing , Rao, Linghui , Gauza, Sebastian and Wu, Shin-Tson(2010) 'Optimisation of electrode structure to improve the electro-optic characteristics of liquid crystal display based on the Kerr effect', Liquid Crystals, 37: 2, 201 — 208
To link to this Article: DOI: 10.1080/02678290903494601
URL: http://dx.doi.org/10.1080/02678290903494601

Liquid Crystals,
Vol. 37, No. 2, February 2010, 201–208

Taylor & Francis
Taylor & Francis Group

Optimisation of electrode structure to improve the electro-optic characteristics of liquid crystal display based on the Kerr effect

Sukin Yoon[a], Miyoung Kim[a], Min Su Kim[a], Byeong Gyun Kang[a], Mi-Kyung Kim[a], Anoop Kumar Srivastava[a], Seung Hee Lee[a]*, Zhibing Ge[b], Linghui Rao[b], Sebastian Gauza[b] and Shin-Tson Wu[b]

[a]*Polymer BIN Fusion Research Center, Department of Polymer Nano Science Engineering, Chonbuk National University, Chonju, Chonbuk 561-756, Korea;* [b]*College of Optics and Photonics, University of Central Florida, Orlando, FL 32816, USA*

(Received 30 October 2009; final version received 17 November 2009)

Liquid crystal displays based on the Kerr effect are emerging because of their attractive features, such as symmetric viewing angle, no need for alignment layer, and sub-millisecond response time. However, high operating voltage and low optical efficiency remain as challenges to be overcome. Here, we propose a new cell structure with a protrusion shape of electrode and a driving scheme using two transistors to reduce operating voltage and enhance light efficiency. Confirming simulation results are obtained.

Keywords: liquid crystal display; blue phase; simulation; in-plane switching

1. Introduction

Recently, all large screen liquid crystal displays (LCDs) over 30 inches show high image quality even at off-normal axis owing to adoption of wide-view approaches, such as patterned vertical alignment [1], multi-domain vertical alignment [2], in-plane switching (IPS) [3], and fringe-field switching [4–7]. However, all these devices require molecular alignment layers on the top and bottom substrates, and some even need surface treatment such as a rubbing process. Another intrinsic demerit of these LCDs is that their response time is in the millisecond range, so that image blur occurs when displaying fast-moving images. This motion blurring can be improved by adopting some driving techniques, e.g. overdrive and undershoot voltage [8], blinking or scanning backlight, and high frame frequency [8–10]. However, these approaches increase production cost.

Polymer-stabilised blue phase liquid crystal (BPLC) or nanostructured LC technology is emerging [11–17] because of its fast response time, wide viewing angle and simple fabrication process. Moreover, polymer-stabilised BPLCs are optically isotropic at the voltage-off state; no rubbing process is required. Hence, this is a great advantage from a fabrication viewpoint. Nevertheless, high operating voltage and low optical efficiency remain as major challenges to be overcome [18]. In order to lower the operating voltage, materials with a large Kerr constant (K) and wall-shaped electrode structure have been proposed. On the wall-shaped electrode approach, the electrode height is the same as the cell gap [19]. In reality, fabricating such wall-shape electrodes seems quite difficult; however, the elliptic-like or semi spherical-like shape of electrode with a height of about 1–3 μm can be made fairly easily with the help of organic resin [20].

In this paper, we analyse the electro-optic characteristics of a general polymer-stabilised BPLC display driven by in-plane electric fields and propose various cell structures to overcome the high operating voltage and low optical efficiency by numerical simulations.

2. Switching principle of the device

From a macroscopic viewpoint, the electro-optic characteristics of a polymer-stabilised BPLC are based on the Kerr effect, which is a type of quadratic electro-optic effect caused by field-induced ordering of polar molecules. The induced birefringence of polymer-stabilised BPLC (Δn_i) can be expressed as

$$\Delta n_i = \lambda K E^2 \tag{1}$$

where $\boldsymbol{E}$ is applied electric field, and λ and K represent the wavelength and Kerr constant, respectively. This indicates that a higher Kerr constant and applied electric field would lead to a higher induced birefringence.

In order to utilise polymer-stabilised BPLC for display applications, the LC cell is usually sandwiched between crossed polarisers. In the voltage-off state, the cell appears black because the LC is optically isotropic. In order to induce birefringence effectively, the device should be driven by an in-plane electric field. Therefore, the normalised transmittance (T) of the

*Corresponding author. Email: lsh1@chonbuk.ac.kr

ISSN 0267-8292 print/ISSN 1366-5855 online

DOI: 10.1080/02678290903494601
http://www.informaworld.com

device associated with the induced phase retardation can be described as follows;

$$T = \sin^2 2\psi \times \sin^2(\pi d_i \Delta n_i(V)/\lambda) \qquad (2)$$

where ψ is the angle between the transmission axis of the polariser and the induced optic axis of the LC director, and d_i is the LC layer thickness associated with the induced birefringence. In general, the induced birefringence is concentrated near the electrodes. For maximum transmission, ψ and $d_i\Delta n_i$ should be equal to 45° and $\lambda/2$, respectively.

To simulate the electro-optic characteristics of a polymer-stabilised BPLC cell, we have used the commercially available software 'TechWiz LCD' (Sanayi system, Korea) to calculate the induced birefringence by Kerr effect.

3. Results and discussion

Before we present the new electrode structures for enhancing the electro-optical properties of a BPLC display, we investigate voltage-dependent transmittance behaviour of the BPLC cell based on the conventional IPS structure shown in Figure 1. Both common and pixel electrodes exist only at the bottom substrate with thickness (t) of 0.04 μm (we call this the IPS cell). Here, the electrode width (W) and pattern spacing (L) between electrodes are 4 μm and 8 μm, respectively, while the LC cell gap (d) is 6 μm. For the purpose of numerical simulation, we assume that K of polymer-stabilised BPLC, Δn and $\Delta\varepsilon$ of the host LC are 5.5×10^{-10} m/V^2, 0.150, and 4.5, respectively.

Figure 2 shows the driving schemes and corresponding voltage-dependent transmittance (V–T) curves. In the conventional driving scheme shown in Figure 2(a), the amplitude of pixel (PXL) electrode

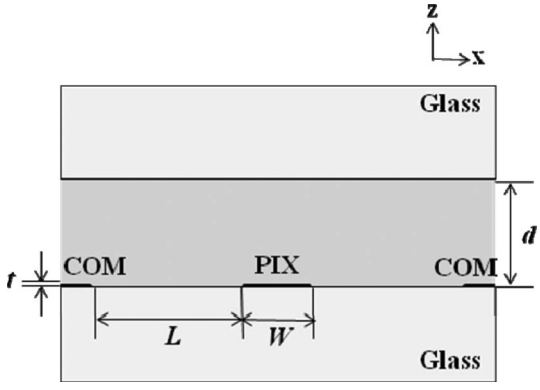

Figure 1. Cross-sectional view of conventional polymer-stabilised blue phase liquid crystal cell in in-plane switching mode.

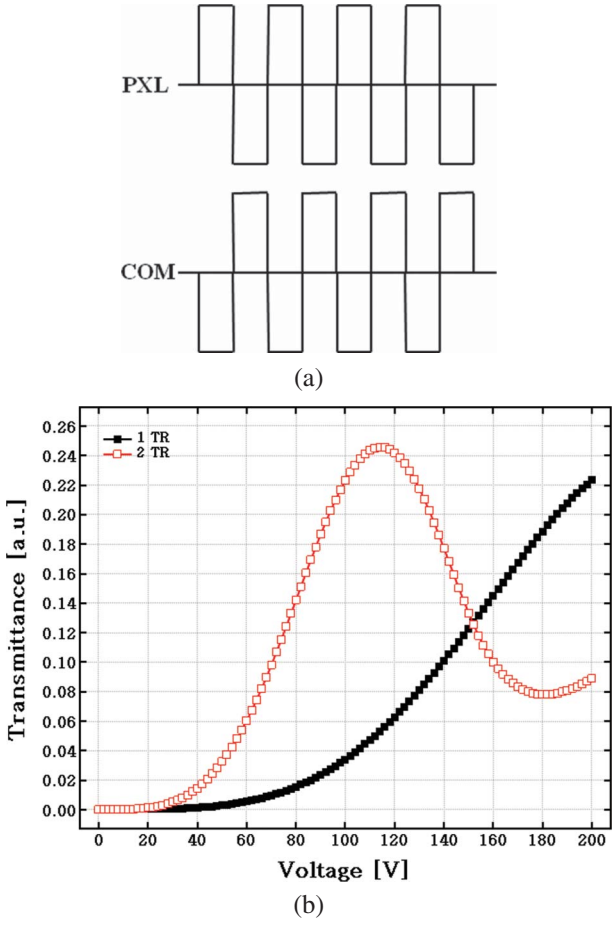

Figure 2. (a) Driving schemes and (b) the calculated voltage-dependent transmittance (V–T) curves corresponding to the driving scheme.

voltage is controlled via only one transistor (TR) in each pixel while the common (COM) voltage is fixed. Here, we propose a new driving scheme which controls PXL and COM electrode voltages separately using two TRs in one pixel. In the 2TR driving scheme, the PXL and COM electrodes are biased at positive/negative voltage pulse and negative/positive voltage pulse, respectively. Referring to Figure 2(b), the 2TR driving scheme exhibits an approx twice as low operating voltage than the 1TR because of its much higher electric fields. Therefore, we have used the 2TR driving scheme for the following simulations.

Figure 3 shows the calculated V–T distributions, horizontal electric-field (E_x) pattern and effect of transmittance distributions at 114 V on the LC cell. Referring to Figure 3(a), the IPS BPLC cell exhibits high transmittance in the area between PXL and COM electrodes, while it exhibits no transmittance above the electrodes. However, in the area between PXL and COM electrodes, although high transmittance appears as the applied voltage increases, transmittance distribution fluctuates

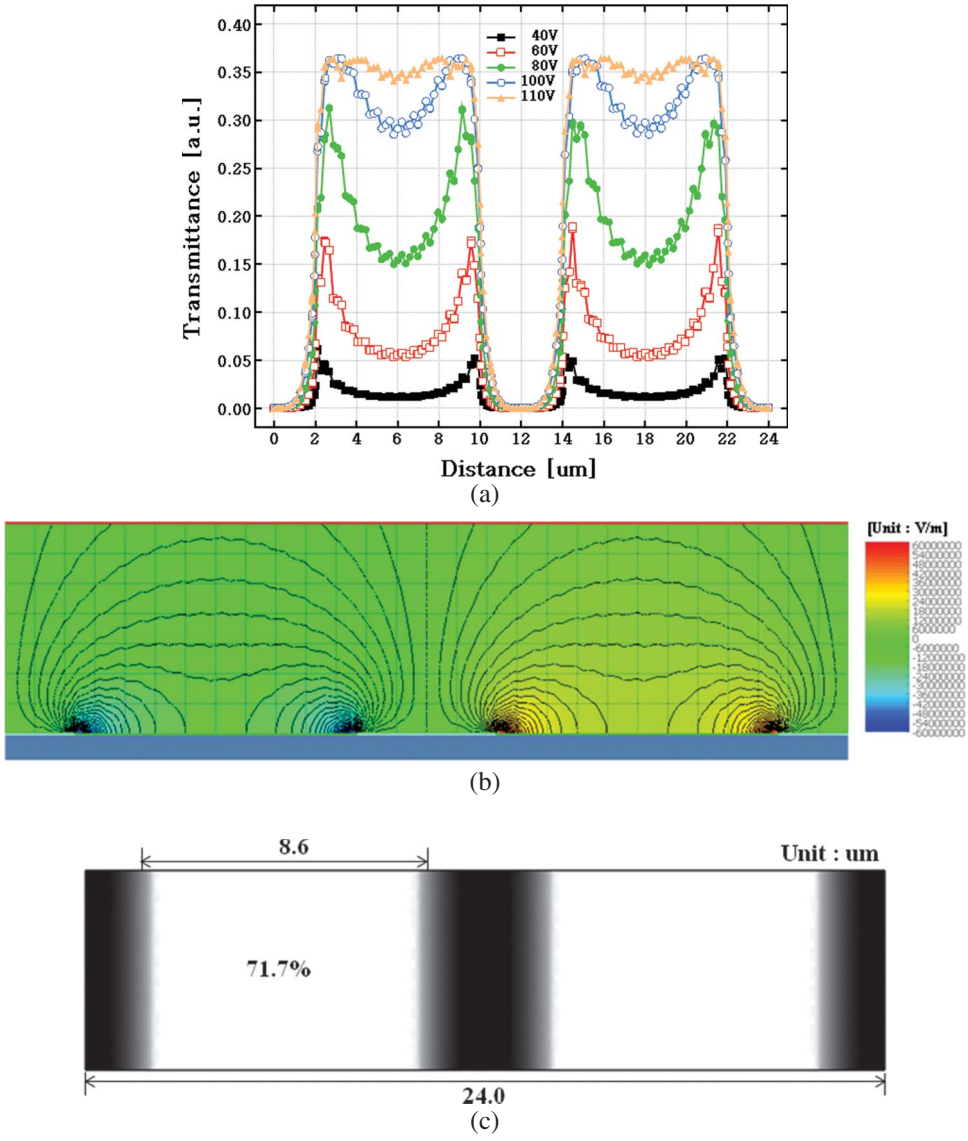

Figure 3. The calculated (a) voltage-dependent transmittance distributions, (b) horizontal *E*-field (E_x) distributions and (c) transmittance distribution at the operating voltage $V_{op} = 114$ V in the cell structure.

at high voltages because of the difference of the induced birefringence Δn_i at each position. Figure 3(b) explains the cause of different Δn_i at each position. The strong E_x distribution concentrates locally at the edges of electrodes, and weak E_x distribution is widely distributed on the centre area between electrodes. Therefore, total transmittance is reduced because the total retardation $d_i\Delta n_i$ at each position along the *x*-axis has different values in this structure. Additionally, since no horizontal field appears on top of the electrodes, the transmittance remains very low even over the operating voltage (V_{op}), leading to a reduced aperture ratio. According to Figure 3(c), its aperture ratio is 71.7%, if we define the aperture as where the transmittance exceeds 25% of the maximum intensity.

In order to investigate the trend of *V–T* characteristics according to various electrode width/pattern spacing (*W*/*L*) ratio parameters, we have simulated various parameters of IPS cell structure. Figure 4 shows the calculated *V–T* curves corresponding to the *W*/*L* parameter. According to Figure 4, a smaller pattern spacing *L* with the same *W*/*L* parameter leads to a lower operating voltage. However, transmittance is decreased because of the reduction of electric field flux caused by the narrower electrode width *W*, resulting in decreased LC layer thickness with induced birefringence (d_i). In other words, although a smaller *L* generates higher electric fields, which subsequently induces birefringence more easily, transmittance is decreased by the effect of $d_i\Delta n_i$ since the smaller *W* under the same

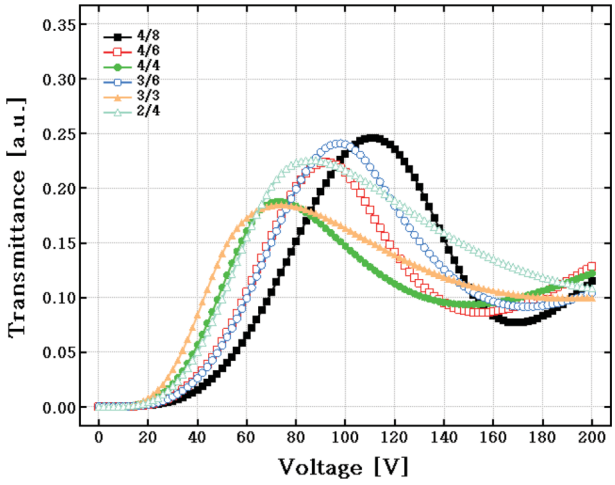

Figure 4. The calculated voltage-dependent transmittance curves corresponding to the electrode width (W)/electrode pattern spacing (L) parameters.

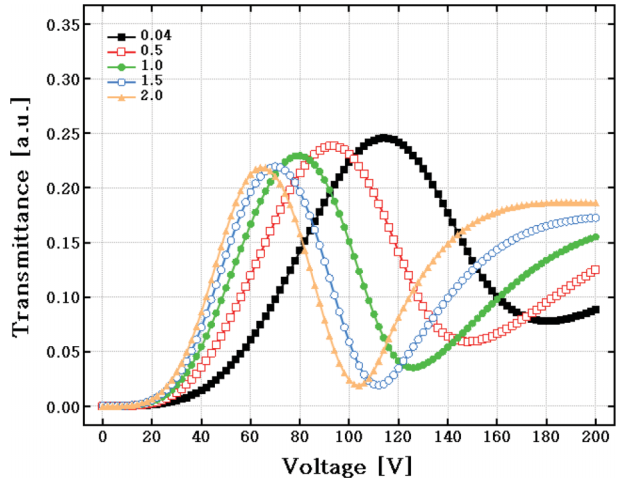

Figure 5. The calculated voltage-dependent transmittance curves according to the electrode thickness t. Here, t was varied from 0.04 to 2 μm

W/L condition reduces the LC layer thickness with the induced birefringence. Furthermore, a smaller pattern spacing L with the constant electrode width W also decreases the transmittance due to the increased portion of dark area on the electrodes. Therefore, in order to reduce operating voltage, the pattern spacing L should be reduced. However, the reduced pattern spacing L would cause a low transmittance as we mention above. Therefore, in order to improve transmittance efficiency it is necessary to extend the aperture region by generating E_x on the electrodes and reducing imbalance of $d_i\Delta n_i$ at each position in the area between the patterned electrodes which is caused by the different E_x distributions. In this paper, the effect of electrode shape was investigated in order to find the optimal electrode shape for improving the aperture ratio, which in turn improves the transmittance efficiency of BPLC cell. In addition, to lower the operating voltage, we optimise the W/L parameter by designing proper electrode shapes.

Figure 5 shows the calculated V–T curves as a function of the electrode thickness (t). Here, t is varied from 0.04 to 2 μm. The taper angle of electrode is fixed at 89° and the cell structure is based on $W = 4$ μm, $L = 8$ μm and $d = 6$ μm. Practically, although some of electrode shapes used in our simulation are very difficult to form on indium tin oxide (ITO), we have assumed the use of ITO material for the patterned electrodes because the structures can be fabricated by patterning the electrodes over organic resin protrusion in the real process.

According to Figure 5, as the electrode gets thicker, the operating voltage decreases because of the stronger E_x caused by the increased side surface of electrode. However, in contrast, its transmittance is reduced because the retardation according to the induced birefringence, which is caused by the E_x above the electrode surface, becomes relatively smaller by the reduction of BPLC thickness as the electrode thickness increases. Finally, the retardation on the top surface of the electrodes over 2 μm of electrode thickness can be neglected.

Figure 6 shows the calculated V–T curves as a function of the electrode taper angle. The electrode in each structure has a different taper angle and a maximum thickness of 2 μm. In the structure whose taper angle is less than 45°, its thickness is also reduced according to the taper angle as shown in Figure 6(b). Referring to Figure 6(a), the larger taper angle leads to a lower operating voltage. However, at 45° of electrode taper angle, which has a structure like pyramid, it shows the highest transmittance efficiency. Above 45° of taper angle, since the electrode thickness is saturated at 2 μm, the transmittance efficiency starts to decrease for the aforementioned reason.

Therefore, it is clear that an electrode with a pyramid shape which has no flat top surface is effective to extend the aperture ratio of the electrodes. Figure 7 shows the calculated V–T curves for various types of pyramid structures, such as ellipse, sine-curved, linear, S-shaped, reversed sine-curved, and reversed-ellipse by different processes for generating electrode patterns. All the structures discussed here have electrode width $W = 4$ μm, electrode thickness $t = 2$ μm, pattern spacing $L = 8$ μm and cell gap $d = 6$ μm, while each structure has a different electrode shape as shown in Figure 7(a).

According to Figure 7(b), the reversed ellipse-shaped structure exhibits the highest transmittance efficiency, that is to say, the pattern with the sharpened top is the most effective for improving aperture

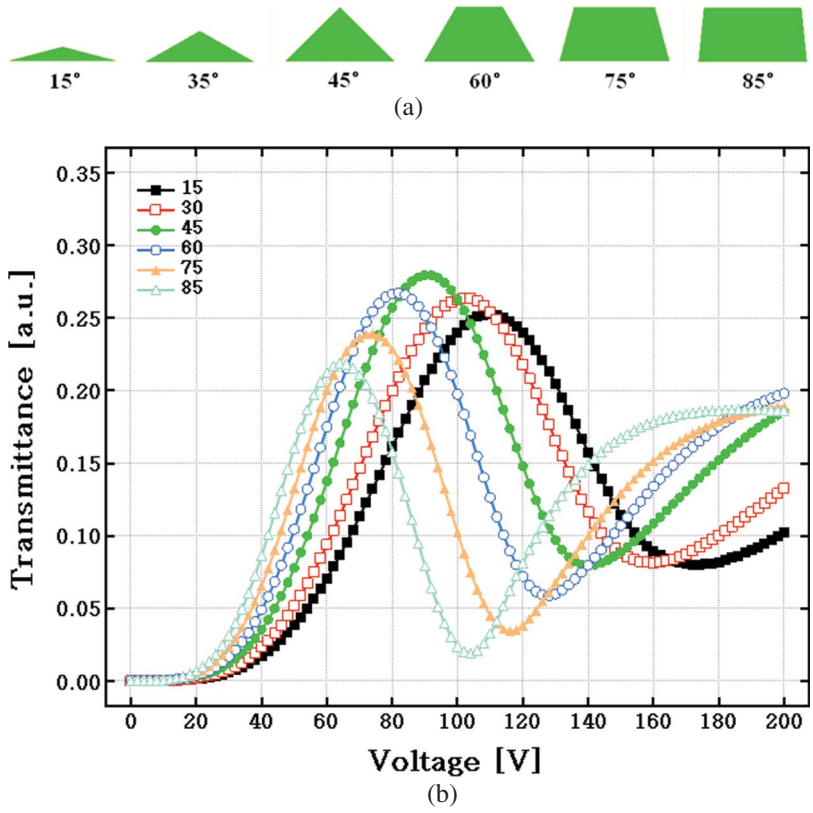

Figure 6. (a) The calculated voltage-dependent transmittance curves according to the electrode taper angle and (b) the electrode shapes.

ratio. Referring to Figure 7(c), the aperture ratio of the cell which has the reversed ellipse-shaped electrodes reaches 98.3%, assuming the aperture region with more than 25% of the maximum intensity.

With the reversed ellipse-shaped electrode, we have simulated *V–T* curves for different types of cell structures with various *W*/*L* ratios. Although the reversed ellipse-shaped electrode shows the highest transmittance efficiency, we also include S-shape and reversed sine-shape for comparison in case the reversed ellipse-shape electrode loses its sharp top during device fabrication.

Figure 8 shows the calculated *V–T* curves corresponding to the *W*/*L* parameter. According to Figure 8, in the proposed structure, smaller pattern spacing *L* with either the same *W*/*L* ratio or the constant electrode width *W* leads to a lower operating voltage with improvement of transmittance efficiency. In a conventional structure with flat top surface of electrode, as pattern spacing *L* gets smaller, the vertical electric field E_z gets stronger, instead of E_x. However, our new structure with a sharp top surface of electrode generates a higher E_x as pattern spacing *L* gets smaller.

Furthermore, smaller pattern spacing *L* with the same W/L ratio helps to minimise the non-uniform $d_i\Delta n_i$ at different positions of the cell. Figure 9 shows the transmittance distribution at the operating voltage of (a) $W/L = 4/8$ at 98 V, (b) $W/L = 3/6$ at 76 V, and (c) $W/L = 2/4$ at 52 V for the reversed ellipse-shape electrode configuration. Referring to Figure 9, a smaller transmittance difference caused by different $d_i\Delta n_i$ at the centre and edges of pattern spacing is observed, as compared with a conventional cell. In addition, a smaller pattern spacing *L* exhibits a larger transmittance efficiency above the electrodes.

In addition to the above-mentioned electrode configuration for enhancing horizontal electric fields, another effective method to lower the operating voltage is to employ BPLC with a large Kerr constant [21, 22]. The Kerr constant is governed by the intrinsic birefringence, dielectric anisotropy of the LC composite, and the cholesteric pitch length as [23]:

$$K \sim \frac{\Delta n_i}{\lambda E^2} \approx \Delta n \cdot \Delta\varepsilon \frac{\varepsilon_o P^2}{k\lambda(2\pi)^2}. \qquad (3)$$

Here, Δn_i is the induced birefringence, λ is the wavelength, *E* is the electric field; Δn, $\Delta\varepsilon$ and *k* are the intrinsic birefringence, dielectric anisotropy, and elastic constant of the host LC material. The pitch length *P* is related to the Bragg reflection wavelength λ_B as [24]:

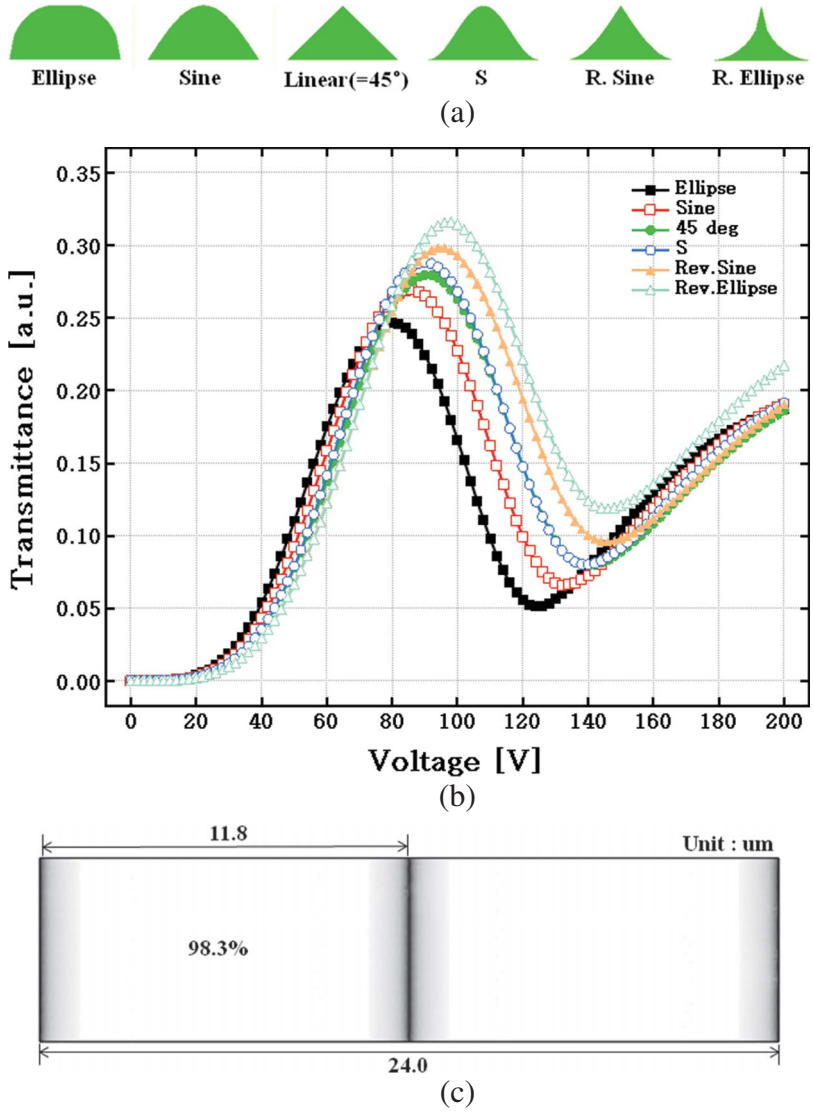

Figure 7. (a) The variation of electrode shape and (b) the calculated voltage-dependent transmittance curves according to the variation electrode shape, (c) transmittance distribution of the cell with the reversed ellipse-shaped electrode.

$$\lambda_B = \langle n \rangle P, \tag{4}$$

where $\langle n \rangle$ is the average refractive index of the LC. From Equation (3), to enhance the Kerr constant, the LC composite with large optical and dielectric anisotropies, long pitch length, and small elastic constant is favourable. In particular, the pitch length has a quadratic effect on the Kerr constant. In a BPLC, we normally design P to shift the Bragg reflection to the ultraviolet region so that it will not affect the display performance in the visible region. On the other hand, if we design λ_B to occur at a near infrared wavelength by increasing P, then the Kerr constant will be increased dramatically. However, higher order Bragg reflections could occur in the visible region. For display applications, any reflection band in the visible spectral region should be avoided. Another concern for increasing pitch length is the slower response of the BPLC device. The response time of a BPLC is related to the pitch length as [24]:

$$\tau \approx \frac{\gamma_1 P^2}{k(2\pi)^2} \tag{5}$$

where γ_1 is the rotational viscosity, and k the elastic constant.

Another controversy exists in the elastic constant of the LC composite. From Equation (3), a small elastic constant is favourable for boosting the Kerr constant, but has a negative effect on response time. Therefore, to optimise the BPLC material and device performances, a delicate balance between operating voltage, transmittance, and response time should be all taken into consideration.

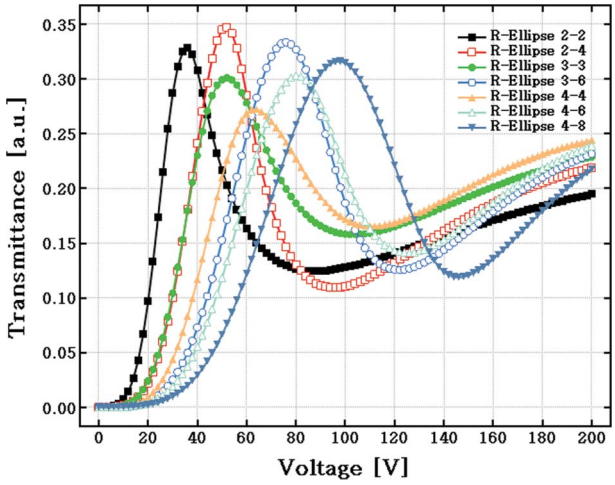

(a)

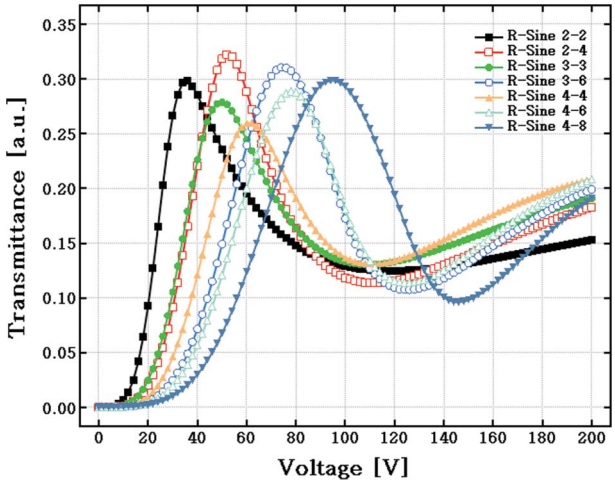

(b)

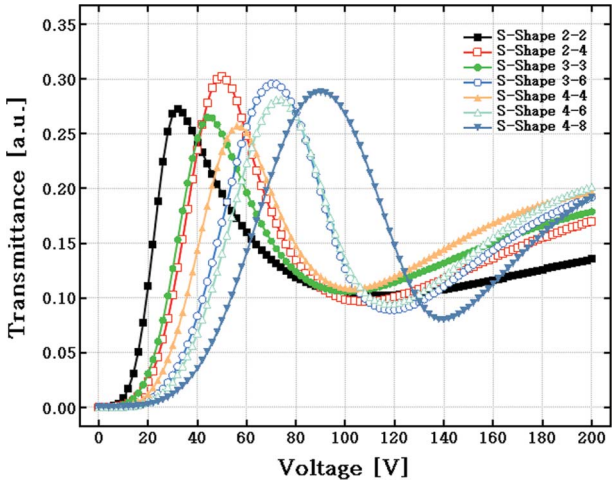

(c)

Figure 8. The calculated voltage-dependent transmittance curves corresponding to the electrode width (W)/electrode pattern spacing (L) parameters of the proposed structure: (a) the reversed ellipse-shaped, (b) reversed sine-shaped, and (c) S-shaped.

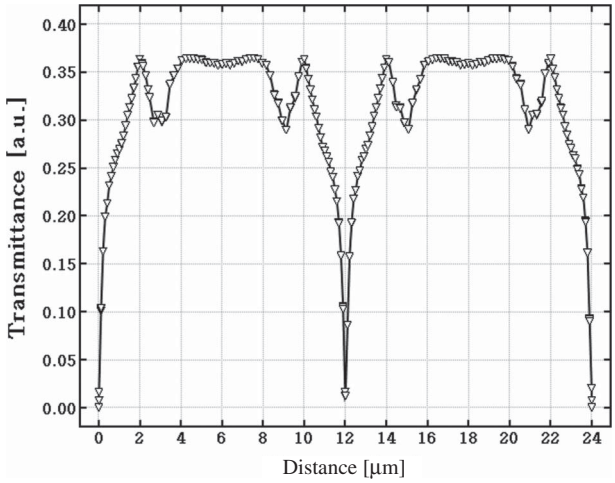

(a)

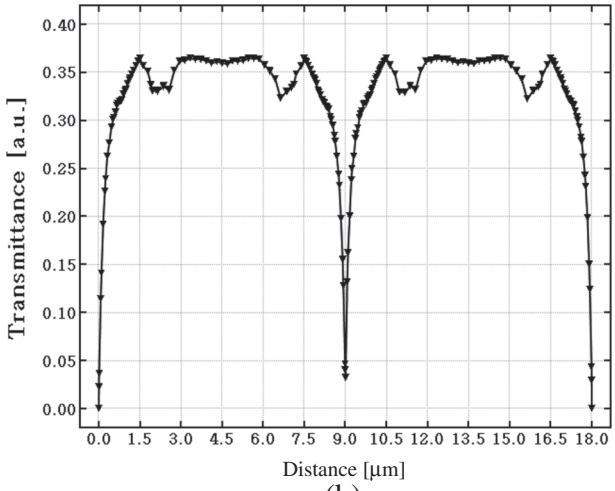

(b)

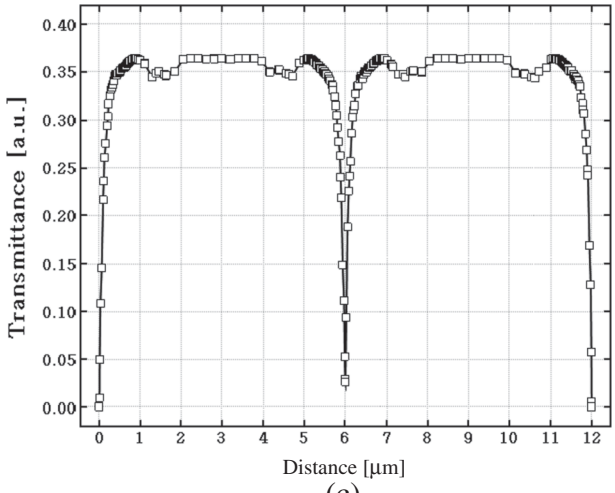

(c)

Figure 9. The transmittance distribution at the operation voltage (the reversed ellipse-shaped): (a) $W/L = 4/8$ at 98 V, (b) $W/L = 3/6$ at 76 V, and (c) $W/L = 2/4$ at 52 V.

4. Conclusion

In a conventional IPS-type BPLC display, low transmittance efficiency and high operating voltage occur because a horizontal electric field is not generated above the electrodes and the field is not strong between pixel and common electrodes. Here, we have proposed a new cell structure with a two-transistor driving scheme to overcome the low transmittance efficiency of the conventional IPS-type BPLC display. The proposed structure has an electrode with a sharp shape at the top. Practically, the proposed electrode structure can be formed by deposition of the electrode on the protrusion etched by isotropic etching process. As a result, the proposed cell structure gives an aperture ratio over 95%, which helps to reduce the operating voltage by 25%.

Acknowledgement

This work was supported by WCU program through MEST (R31-2008-000-20029-0).

References

[1] Kim, K.H.; Lee, K.H.; Park, S.B.; Song, J.K.; Kim, S.N.; Souk, J.H. *Proc. Asia Display* **1998**, 383–386,
[2] Takeda, A.; Kataoka, S.; Sasaki, T.; Chida, H.; Tsuda, H.; Ohmuro, K.; Sasabayashi, T.; Koike, Y.; Okamoto, K. *SID Int. Symp. Digest Tech. Papers* **1998**, *29*, 1077–1080.
[3] Oh-e, M.; Kondo, K. *Appl. Phys. Lett.* **1995**, *67*, 3895–3897.
[4] Lee, S.H.; Lee, S.L.; Kim, H.Y. *Appl. Phys. Lett.* **1998**, *73*, 2881–2883.
[5] Lee, S.H.; Lee, S.L.; Kim, H.Y. *Proc. Asia Display* **1998**, 371–374,
[6] Lee, S.H.; Lee, S.L.; Kim, H.Y.; Eom, T.Y. *SID Int. Symp. Digest Tech. Papers* **1999**, *30*, 202–205.
[7] Pan, H.; Feng, X.; Daly, S. *SID Int. Symp. Digest Tech. Papers* **2005**, *36*, 1590–1593.
[8] Jung, J.H.; Park, J.W.; Kim, M.; Lim, Y.J.; Chung, T.J.; Lee, S.H. *Proc. IDRC* **2008**, 158–160,
[9] Kurita, T. *SID Int. Symp. Digest Tech. Papers*, **2001**, *32*, 986–989.
[10] Lee, S.W.; Kwon, S.; Kim, M.; Souk, J.; Kim, S.S. *SID Int. Symp. Digest Tech. Papers* **2005**, *36*, 1496–1499.
[11] Kikuchi, H.; Higuchi, H.; Haseba, T.; Iwata, T. *SID Int. Symp. Digest Tech. Papers* **2007**, *38*, 1737–1740.
[12] Kikuchi, H.; Yokota, M.; Hisakado, Y.; Yang, H.; Kajiyama, T. *Nat. Mater.* **2002**, *1*, 64–68.
[13] Hisakado, Y.; Kikuchi, H.; Nagamura, T.; Kajiyama, T. *Adv. Mater.* **2005**, *17*, 96–98.
[14] Haseba, Y.; Kikuchi, H. *J. Soc. Inf. Disp.* **2006**, *14*, 551–556.
[15] Kikuchi, H.; Higuchi, H.; Haseba, Y.; Iwata, T. *SID Int. Symp. Digest Tech. Papers* **2007**, *38*, 1737–1740.
[16] Choi, S.W.; Yamamoto, S.; Haseba, Y.; Higuchi, H.; Kikuchi, H. *Appl. Phys. Lett.* **2008**, *92*, 043119.
[17] Yang, Y.C.; Bao, R.; Li, K.; Yang, D.K. *SID Int. Symp. Digest Tech. Papers* **2009**, *40*, 586–589.
[18] Ge, Z.; Gauza, S.; Jiao, M.; Xianyu, H.; Wu, S.T. *Appl. Phys. Lett.* **2009**, *94*, 101104.
[19] Kim, M.S.; Kim, M.; Jung, J.H.; Ha, K.S.; Yoon, S.; Song, E.G.; Srivastava, A.K.; Choi, S-W.; Lee, G-D.; Lee, S.H. *SID Int. Symp. Digest Tech. Papers* **2009**, *40*, 1615–1618.
[20] Zhu, X.; Ge, Z.; Wu, T.X.; Wu, S.T. *J. Display Technol.* **2005**, *1*, 15–29.
[21] Schadt, M. *J. Chem. Phys.* **1977**, *67*, 210–216.
[22] Ge, Z.; Rao, L.; Gauza, S.; Wu, S.T. *J. Display Technol.* **2009**, *5*, 250–256.
[23] Gerber, P.R. *Mol. Cryst. Liq. Cryst.* **1985**, *116*, 197–206.
[24] Wu, S.T.; Yang, D.K. *Reflective Liquid Crystal Displays*; Wiley: New York, 2001.